



## Research Article

# Investigation of synergetic effect of adsorption and photocatalysis for the removal of tetracycline by BiFeO<sub>3</sub> immobilized on copolymer seeds

Esra BİLGİN ŞİMŞEK<sup>\*</sup>, Zeynep BALTA

Department of Chemical Engineering, Yalova University, Yalova, Türkiye

## ARTICLE INFO

### Article history

Received: 02 November 2021

Revised: 06 February 2022

Accepted: 09 March 2022

### Key words:

Adsorption; Antibiotic; BiFeO<sub>3</sub>; Perovskite; Photocatalysis

## ABSTRACT

The utilization of powdered photocatalysts can cause problems such as agglomeration and difficulty in separation in conventional applications. In this work, deposition of photocatalyst particles on a co-polymeric network was suggested to solve this issue. For this purpose, ferrite type perovskite BiFeO<sub>3</sub> particles were immobilized on the sulphonated polystyrene-divinyl benzene seeds via a facile impregnation process and the heterostructured catalyst (BFO@co-STR/DVB) exhibited boosted removal performance towards tetracycline antibiotic. The co-polymer itself showed attractive adsorption (93% removal) towards tetracycline due to the robust  $\pi$ - $\pi$  stacking or hydrophobic relationship. The photocatalytic performance of optimal BFO@co-STR/DVB catalyst had the greatest value of apparent rate constant (0.037 min<sup>-1</sup>), which was 6.16 times higher than that for bare BiFeO<sub>3</sub> (0.006 min<sup>-1</sup>). Moreover, the heterostructured photocatalyst displayed the highest catalytic efficiency as 98.5% which was mainly assigned to the synergetic effect of adsorption and photocatalysis. Therefore, detailed adsorption mechanism was examined by applying three kinetic models and the pseudo-second order model ( $q_e=88.9$  mg/g;  $R^2=0.993$ ) was fitted well describing well the adsorption. The impact of perovskite amount on the polymer structure was also investigated. Apart from tetracycline molecule, the photocatalytic activity of the heterostructured catalyst with respect to different pharmaceutical (isoniazid) was also investigated and the adsorptive removal of isoniazid over the co-STR/DVB polymer was calculated as 80.0% while it significantly increased to 98.2% in the BFO@co-STR/DVB photocatalytic system. This study demonstrated the effective utilization of the perovskite deposited co-polymeric network in the field of “photocatalysis”.

**Cite this article as:** Bilgin Şimşek E, Balta Z. Investigation of synergetic effect of adsorption and photocatalysis for the removal of tetracycline by BiFeO<sub>3</sub> immobilized on copolymer seeds. Environ Res Tec 2022;5:2:128–136.

## INTRODUCTION

In recent years, ferrite type perovskite materials have attracted great attentions due to their excellent characteristics in the field of photocatalysis. Among these perovskites,

bismuth ferrite (BiFeO<sub>3</sub>) has been a great interest, because of its high chemical stability, magnetoelectric and optical properties [1]. The rhombohedral distorted BiFeO<sub>3</sub> structure has been investigated as multiferroic material which have ferroelectric ( $T_c=1103$  K) and antiferromagnetic

\*Corresponding author.

\*E-mail address: esrabilgin622@gmail.com



( $T_N=643$  K) characteristics over a wide temperature range [2]. The band gap of  $\text{BiFeO}_3$  (2.1–2.6 eV) lying in the visible region of the solar spectrum enables it to be applied as photovoltaic cell and photocatalyst [3]. Additionally,  $\text{BiFeO}_3$  has been also used as Fenton-catalyst which can effectively catalyze the decomposition of  $\text{H}_2\text{O}_2$  into  $\bullet\text{OH}$  for the degradation of organic pollutants in heterogeneous processes [4].

However, the powder forms of the perovskites can bring some drawbacks such as agglomeration and difficulty in separation which strongly restricts their catalytic activities as well as industrial utilizations. In addition, the bulk perovskites show relatively low surface areas, limiting their interaction with the target molecules. To address these problems, the usage of supporting materials for perovskite oxides has been concerned as an effective strategy. The selection of support is essential as the physicochemical features and catalytic activities of the photocatalysts are closely associated with the type and nature of the matrix. For example, Wu et al. [5] investigated the effect of various supports ( $\text{Al}_2\text{O}_3$ ,  $\text{TiO}_2$ ,  $\text{CeO}_2$ , and  $\text{SiO}_2$ ) for the  $\text{LaFeO}_3$  particles and applied for the degradation of Acid Orange 7. Authors stated that the perovskite supported on  $\text{Al}_2\text{O}_3$  exhibited the highest catalytic activity ascribed to its large surface area, oxygen vacancies, suitable redox property, and fast electron mobility. Li et al. [6] tested different mesoporous silica supports for  $\text{LaFeO}_3$  for the catalytic oxidation of rhodamine B and concluded as the roles of the support were absorbing dye molecules from solution to the pores (i) and then transferring them from the pores to the active site (ii). Alpay et al. [7] demonstrated that the commercial polystyrene based resin (Diaion<sup>TM</sup> HP21) served as a well matrix for the deposition of  $\text{LaFeO}_3$  perovskites and the composite catalyst displayed improved visible light absorption as well as high photocatalytic, degradation activity towards many dyes and antibiotics.

Porous polymeric materials with tunable pore size and controllable morphology have been effectively used as matrices for the deposition of fine particles [8, 9]. It is well known that the styrene-divinylbenzene co-polymers are mechanically and chemically stable as well as they have high adsorption abilities towards many organics [10, 11]. Also, their distinct features of including abundant surface functional groups enable them to be applied as efficient adsorbents for binding organic molecules [12]. Besides, the sulphonated aromatic polymers have higher ion exchange capacity and water absorption features, and they can be effectively utilized in wastewater treatment owing to their abundant sulphonic acid groups [13, 14]. The cross-linked polystyrene co-divinyl benzene has many phenyl rings which can be easily functionalized with sulfonated groups [15]. Therefore, it was hypothesized that the sulfonated styrene-divinylbenzene co-polymers can be a good candidate for the adsorption of the organics and can serve as a matrix for the immobilization of perovskite particles.

Inspired by these perspectives, in this work,  $\text{BiFeO}_3$  perovskite particles were immobilized over the co-polymer surface through wet impregnation method. To the best of our knowledge, there has been no study reported yet about deposition of  $\text{BiFeO}_3$  particles over polymeric substances which might be ideal support for powdered photocatalysts. The as-prepared heterostructure catalyst was applied to the photocatalytic degradation of tetracycline antibiotic under visible light illumination. The enhancement of the photocatalytic activity was attributed to the synergistic effect of adsorption and photocatalysis. In addition, the loading amount of  $\text{BiFeO}_3$  over the resin was investigated. Besides, the photoactivity was tested towards another pharmaceutical namely isoniazid which is known as a persistent drug. We report for the first time on the facile fabrication of co-polymer supported  $\text{BiFeO}_3$  perovskites, integrating both adsorption and photodegradation to simultaneously improve elimination of pharmaceuticals from water media.

## MATERIALS AND METHODS

### Materials

Bismuth (III) nitrate pentahydrate ( $\text{Bi}(\text{NO}_3)_3 \cdot 5\text{H}_2\text{O}$ , 98%) and iron (III) chloride ( $\text{FeCl}_3 \cdot 6\text{H}_2\text{O}$ , 99%) were purchased from Sigma-Aldrich and Lab-Scan Analytical Sciences, respectively. Styrene (Fluka), divinyl benzene (Aldrich), chlorosulfonic acid (99%, Fluka) were purified before use. All other chemicals used in the studies were of analytical reagent grade.

### Preparation of Raw $\text{BiFeO}_3$ Perovskite

Perovskite type  $\text{BiFeO}_3$  particles were prepared by using precipitation method. First, defined amount of  $\text{Bi}(\text{NO}_3)_3 \cdot 5\text{H}_2\text{O}$  was dissolved in 2.5 M  $\text{HNO}_3$  solution. Meanwhile, equal molar amount of  $\text{FeCl}_3 \cdot 6\text{H}_2\text{O}$  was prepared in deionized water. Then, both solutions were mixed and magnetically stirred for 30 min. The solution pH was adjusted to 10 by adding  $\text{NaOH}$  (6 M) and kept stirring for 24 h at room temperature. At the end of the period, the precipitate was filtered and dried 90 °C for 4 h. Finally, the powder was calcined at 600 °C for 3 h. Final product was coded as BFO.

### Preparation of co-Polymer

Styrene-divinyl benzene (STR/DVB) co-polymer beads were synthesized with 50% of cross-linking divinyl benzene. In a typical synthesis, styrene and divinyl benzene were first dissolved in toluene. Alumina and gum arabic emulsifier were prepared in a three-necked round-bottomed flask under nitrogen gas. Then, the mixture of styrene-divinyl benzene was added to the above solution. The polymerization reaction was allowed to continue for 4 h under continuous stirring at 75 °C. The obtained seeds were washed with excess water and dried at 60 °C for overnight. The sulphonation procedure was followed according to the

procedure described in the literature [16]. 10 mL of chlorosulfonic acid was poured into a solution of formamide under constant stirring at 0 °C and the cross-linked polymer beads (2 g) was added to the mixture and kept stirred under reflux conditions for 5 h. The resultant resins were filtered and washed with cold water and acetone. The final seeds were labelled as co-STR/DVB.

#### Immobilization of BiFeO<sub>3</sub> Over co-Polymer Structure

The immobilizing of BiFeO<sub>3</sub> particles on co-STR/DVB structure was performed via impregnation method. Briefly, 5 mg BFO particles mixed with 50 mg of co-STR/DVB seeds (0.2 g). The suspension was mixed at orbital shaker for 48 h. Then, the brown seeds were collected, washed with de-ionized water and subsequently dried at 60 °C overnight. The product was coded as BFO@co-STR/DVB (1:10). In order to examine effect of perovskite ratio, the amount of BFO particles were changed as 10 and 25 mg; the resultant samples were coded as BFO@co-STR/DVB (2:10) and BFO@co-STR/DVB (5:10), respectively.

#### Characterization Tests

The surface morphology and elemental analysis were investigated by scanning electron microscopy (FEI Inc., Inspect S50 SEM, EDAX Octane Prime). The Fourier transfer infrared (FTIR) spectra were obtained on Perkin Elmer Spectrum One using attenuated total reflectance method. X-ray powder diffraction (XRD) data were collected using CuK $\alpha$  radiation (Panalytical X'Pert PRO Model).

#### Adsorption and Photocatalytic Degradation Studies

In order to examine the adsorptive removal of TC-HCl over co-STR/DVB seeds, the adsorption kinetic tests were performed with initial concentration of 10 mg/L at 298 K and pH 6.5. Photocatalytic decomposition of tetracycline (TC-HCl) was investigated under visible light irradiation by using a square-shaped photochemical reactor coupled with two visible metal halide lamps ( $\lambda$ : 400–800 nm). The fan at the bottom of the system was used to decrease the temperature to ambient conditions. For each test, 0.01 g of catalyst was dispersed with 50 mL TC-HCl solution with an initial concentration of 10 mg/L. After 30 min of dark adsorption period, the mixture was exposed to light, and aliquots were taken at time intervals. The residual TC-HCl concentration was analyzed by UV-vis spectrophotometer at the wavelength of 360 nm. The degradation efficiency was calculated by Eq.(1):

$$\text{Degradation\%} = \left[ \frac{(C_0 - C)}{C_0} \right] \times 100 \quad (1)$$

In order to examine the photocatalytic performance of the as-synthesized catalyst towards different pharmaceutical, the degradation of isoniazid was also investigated under similar conditions and the equilibrium isoniazid concentration was determined by UV-Vis spectrophotometer at 262 nm.

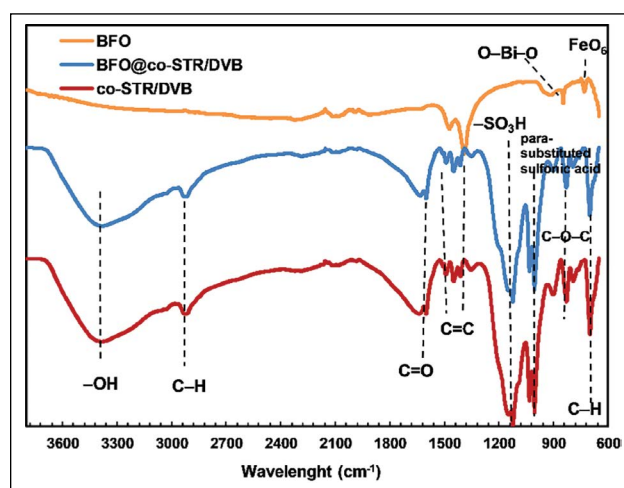


**Figure 1.** FTIR spectra of BFO, BFO@co-STR/DVB and co-STR/DVB samples.

## RESULTS AND DISCUSSION

#### Characterization

In order to examine the surface functional groups after immobilization, FTIR spectra of BFO, BFO@co-STR/DVB and co-STR/DVB samples were obtained, and the results were shown in Figure 1. In the spectrum of bare BFO perovskite, the presence of nitrate ions was observed at nearly 1450 cm<sup>-1</sup> [17] while the absorption bands at 800–900 cm<sup>-1</sup> were assigned to the symmetric stretching vibrations of O–Bi–O in the BiFeO<sub>3</sub> structure [18]. The FTIR spectra of as-synthesized co-polymers confirmed the presence of aromatic ring features of skeletal C=O and C=C in plate-stretching vibrations at 1601 and 1450 cm<sup>-1</sup>, respectively. The peak at 701 cm<sup>-1</sup> was assigned to the bending vibration of the substituted benzene ring (C–H) [19]. The sulfonation was verified from the peaks in the range of 1000–1130 cm<sup>-1</sup>. The band at 1126 cm<sup>-1</sup> was ascribed to the presence of -SO<sub>3</sub>H groups while the band at 1006 cm<sup>-1</sup> indicated the vibrations of the aromatic ring released from the para-substituted sulfonic acid [19, 20]. The O–H stretching vibration of water was observed at about 2900–3400 cm<sup>-1</sup>. The peaks at 700 and 831 cm<sup>-1</sup> were assigned to the aromatic ring C–H bend and stretching vibration of C–O–C bonds, respectively. After immobilization of BiFeO<sub>3</sub> particles on co-STR/DVB surface, the peak intensities slightly decreased but the characteristic peaks were still observed confirming that the incorporation of perovskites did not alter the functional groups of bare co-STR/DVB.

X-ray diffraction (XRD) was employed to detect the crystallinity of bare BiFeO<sub>3</sub> perovskite. As shown in Figure 2b, the diffraction peak was well indexed to the standard XRD data of rhombohedral BiFeO<sub>3</sub> (JSPDS file No. 86-1518), indicating successful synthesis of crystal perovskite. Regarding the peak intensities, the sharp peaks at  $2\theta=23.2, 30.2, 32.2, 40.9, 45.0, 50.0, 51.0, 54.2, 55.0$  and  $67.3^\circ$  were related

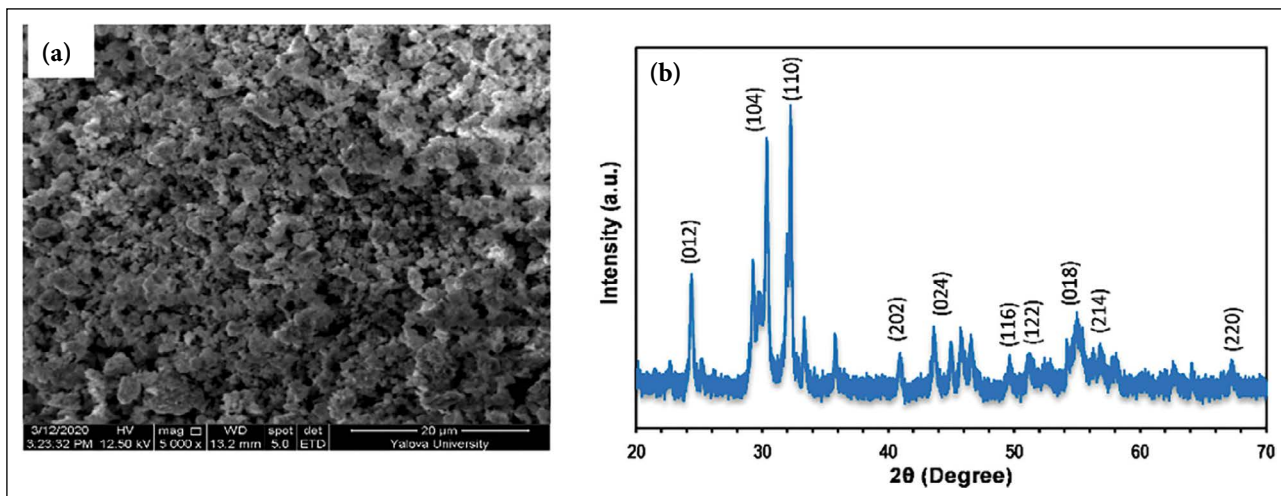


Figure 2. (a) SEM image (a) and XRD spectrum of raw BFO.

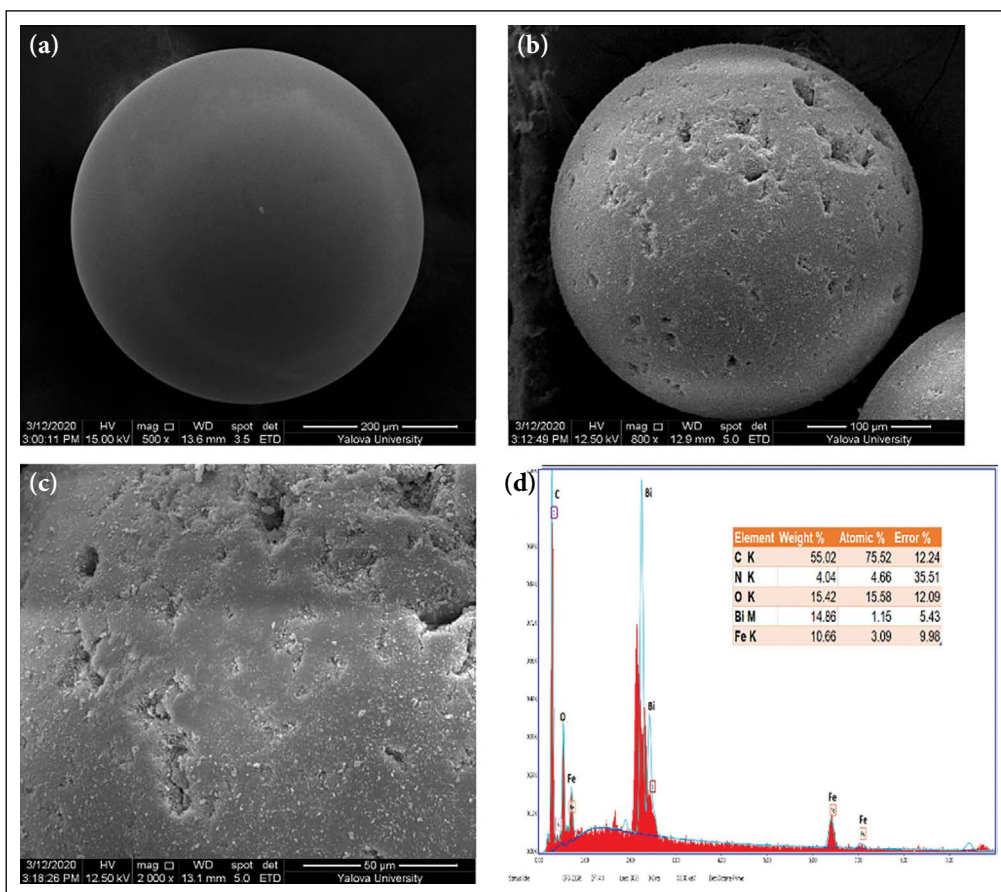
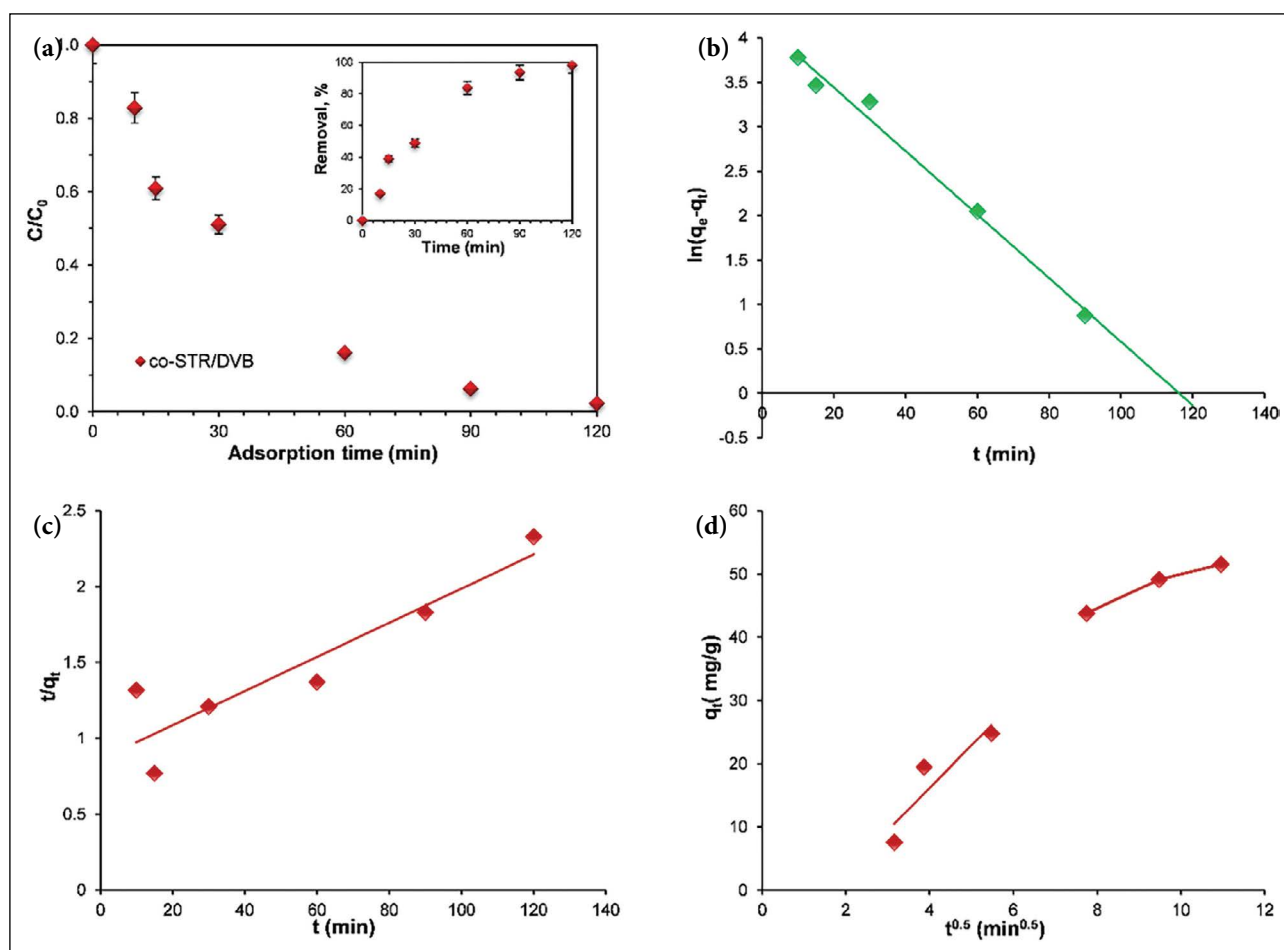


Figure 3. SEM images of raw co-STR/DVB (a), BFO@co-STR/DVB (b, c) and EDS spectrum of BFO@co-STR/DVB composite catalyst.

to their Miller indices (0 1 2), (1 0 4), (1 1 0), (2 0 2), (0 2 4), (1 1 6), (1 2 2), (0 1 8), (2 1 4), (2 2 0), respectively.

Scanning electron microscope (SEM) images of bare BFO, co-STR/DVB and BFO@co-STR/DVB catalysts were presented in Figure 2a, Figure 3. It could be seen that bare BFO

perovskite exhibited irregular polyhedral structure which was in accordance with previous studies [21]. The raw co-STR/DVB sample indicated smooth spherical shape (Fig. 3a) enabling active surface sites to promote the adsorption and degradation towards the tetracycline molecule. After



**Figure 4.** (a) TC-HCl adsorption kinetics, Pseudo-first order (b), Pseudo-second order (c) and Intra-particle diffusion kinetic modelling over co-STR/DVB.

immobilization of  $\text{BiFeO}_3$  perovskites over the co-polymer structure, the spherical shapes morphology of the polymer was not altered (Fig. 3b, c). It was clearly observed that the surface was fully covered with  $\text{BiFeO}_3$  perovskite particles. The particle diameter of the heterostructured catalyst was nearly  $100 \mu\text{m}$ , which was decreased from  $200 \mu\text{m}$  revealing that the impregnation route might impact the particle size of the polymer seeds. The EDX elemental distribution demonstrated the presence of Bi, Fe, O, C and N elements in the composite catalyst verifying effective immobilization of BNQDs into the perovskite framework. The weight ratio of Bi, Fe and O elements were estimated as 14.8%, 10.6% and 15.4%, respectively.

#### Adsorption Kinetics Over co-STR-DVB

The kinetics of adsorption over co-STR/DVB seeds were studied to ensure the required time for equilibrium as well as to find the rate limiting steps of the process. As seen in Figure 4a, at the end of 90 and 120 min, the TC-HCl removal percentages of raw co-STR/DVB were achieved as 93% and 98%, respectively. This robust interaction could

be attributed to the predominant  $\pi$ - $\pi$  stacking or hydrophobic relationship between tetracycline and the co-polymeric structure [11]. The adsorption kinetic data were applied to three kinetic models namely, pseudo-first order, pseudo-second order and Weber-Morris intra-particle diffusion. Table 1 shows the kinetic model parameters with their related correlation coefficients ( $R^2$ ).

The pseudo-first-order kinetic equation is based on the surface physisorption mechanism, and it is defined as:

$$\log(q_e - q_t) = \log q_e - \left(\frac{k_1}{2.303}\right)t \quad (2)$$

where  $q_e$  and  $q_t$  are the amounts of adsorbed TC-HCl (mg/g) at equilibrium and at time  $t$  (min), respectively, and  $k_1$  is the rate constant of pseudo-first-order model ( $\text{min}^{-1}$ ) which was determined from the plots of  $\log(q_e - q_t)$  vs. time (Fig. 4b). From Table 1, the correlation coefficients ( $R^2$ ) for the pseudo-first model were found slightly lower indicating the model is not fitted well the adsorption kinetics of TC-HCl over co-STR/DVB seeds, revealing physical forces were not involved in the adsorption process.

**Table 1.** Adsorption kinetic model constants of co-STR/DVB

$q_e$ (mg/g)	78.54
Pseudo-first order	
$q_e$ (mg/g)	64.01
$k_1$ ( $\text{min}^{-1}$ )	0.082
$R^2$	0.988
Pseudo-second order	
$q_e$ (mg/g)	88.92
$k_2$ (g/mg min)	0.00014
$h$ (mg/g min)	1.160
$R^2$	0.993
Weber–Morris intra-particle diffusion	
$k_{id-1}$ ( $\text{mg/g min}^{0.5}$ )	6.749
$R^2$	0.822
$k_{id-2}$ ( $\text{mg/g min}^{0.5}$ )	2.434
$R^2$	0.972

The pseudo-second-order kinetic model is generally utilized to explain the adsorption mechanisms driven by surface chemisorption process and the model is shown as Eq. (3):

$$\frac{t}{q_t} = \frac{1}{k_2 q_e^2} + \frac{1}{q_e} \quad (3)$$

where  $k_2$  is the second-order rate constant (g/mg min). The  $k_2$  and  $q_e$  values are evaluated from the intercept and the slope of the plot  $t/q_t$  versus  $t$ . Initial adsorption rate ( $h$ , mg/g min) is calculated from Eq. (4):

$$h = k_2 q_e^2 \quad (4)$$

According to the obtained  $R^2$  value and second order rate constant, the second-order model displayed high correlation coefficients ( $R^2=0.993$ ) for of TC-HCl adsorption over co-STR/DVB sample (Fig. 4c). Moreover, the theoretical and experimental adsorption capacities of the pseudo-second-order model were found nearly identical, indicating that this model was more proper for describing that the TC-HCl adsorption was mainly occurred through on  $\pi$ - $\pi$  stacking interactions. Similar observation was reported by Yang et al. [22] and they underlined the fact that electrostatic interactions played minor role in the tetracycline adsorption.

The intra-particle diffusion model was also applied to determine the rate determining step. The model is shown as:

$$q_t = k_{id} t^{0.5} + C \quad (5)$$

where  $q_t$  is the amount of adsorbed TC-HCl at the time (mg/g);  $k_{id}$  ( $\text{mg/g min}^{0.5}$ ) is the Weber-Morris intra-particle-diffusion rate constant;  $t$  is the time (t);  $C$  is intercept (mg/g). The intra-particle-diffusion model parameters including  $k_{id-1}$ ,  $k_{id-2}$  and  $R^2$  were listed in Table 1, and the plots were shown in Figure 4d. The plot of this model exhibited two linearity, verifying the existence of two adsorption

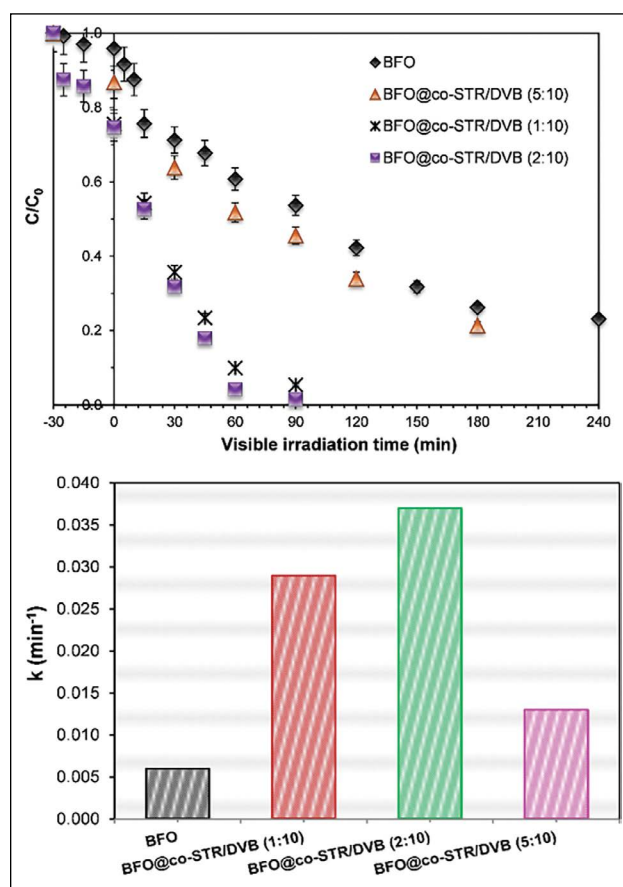


**Figure 5.** Photocatalytic degradation curves and related kinetic constants of BFO and BFO@co-STR/DVB catalysts.

states (phase I-fast adsorption and phase II-slow adsorption) of mass transfer. The first linearity is related with macropore/mesopore diffusion while the second line deals with the micropore diffusion [23]. In the first step, approximately 48% TC-HCl was removed by co-STR/DVB within 30 min which was attributed to the fast utilization of the most active adsorptive areas on the co-polymer surface. Then, 83% of TC-HCl was eliminated within 60 min. The kinetic rate constant of first step ( $k_{id-1}=6.749 \text{ mg/g min}^{0.5}$ ) was found much higher than the second step of adsorption ( $k_{id-2}=2.434 \text{ mg/g min}^{0.5}$ ). Furthermore,  $R^2$  values of the phase I were higher than the phase II suggesting that the external mass transfer could be the rate-limiting step in the adsorption process.

### Photocatalytic Performance Tests of BFO@co-STR/DVB Heterostructure Catalyst

The photocatalytic activities of the BFO@co-STR/DVB heterostructured catalysts were evaluated towards tetracycline degradation from 50 mL of 10 mg/L aqueous solution. Figure 5 revealed the TC-HCL elimination over the photocatalysts, in which the degradation degree of bare BFO was found low (76.9%) even after 240 min of visible irra-

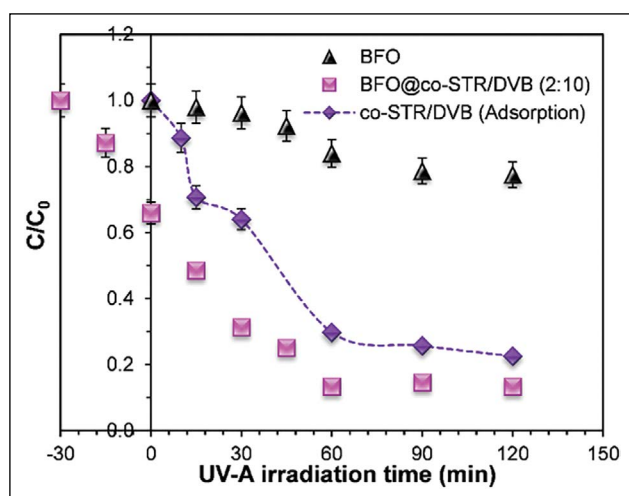


**Figure 6.** Photocatalytic degradation and adsorption curves of towards isoniazid molecule.

diation. This could be owing to its limited light absorption and high recombination of electrons and holes. Moreover, the photodegradation rates over the BFO@co-STR/DVB catalysts increased for the increasing BiFeO<sub>3</sub>: co-STR/DVB ratios of (1:10) and (2:10). Notably, the BFO@co-STR/DVB (2:10) photocatalyst displayed the highest catalytic efficiency as 98.5% while that of for BFO@co-STR/DVB (1:10) was determined as 94.5% at the end of 90 min of irradiation. However, the increasing perovskite content over the heterostructure led to decrease in the removal efficiency and 78.6% photodegradation was calculated for BFO@co-STR/DVB (5:10) catalyst. This could be explained as the increment of the perovskite particles on the surface significantly inhibited the interaction and adsorption of target antibiotic molecules with the co-polymer surface, resulting decrease in the adsorption performance. To confirm this theory, the adsorption performances were also compared. At the end of dark period of 30 min, 24.4%, 25.3% and 13.2% adsorptive removal percentages were observed for BFO@co-STR/DVB (1:10), (2:10) and (5:10) catalysts, respectively, verifying the fact that the interaction of antibiotic molecules was restricted by increased BiFeO<sub>3</sub> particles on the co-polymer surface. Similar phenomenon was observed by Phan et al. [24] who deposited LaFeO<sub>3</sub> particles on acid-modified natural zeolite for the Rhodamine B degradation.

To further elucidate the photodegradation efficiency of the composite catalysts, the degradation kinetic data were applied to the pseudo-first order kinetic equation  $\ln(C/C_0) = -k_{app} \cdot t$ , where  $k_{app}$  shows the apparent first-order reaction rate constant (Fig. 5). The photodegradation performances of the as-prepared samples were quantitatively compared according to the  $k_{app}$  values. It was observed that the BFO@co-STR/DVB (2:10) catalyst had the greatest value of  $k_{app}$  (0.037 min<sup>-1</sup>); in contrast, the rate constants for bare BiFeO<sub>3</sub> was calculated as 0.006

min<sup>-1</sup>, implying that the photodegradation activity of the heterostructured catalyst was 6.16 times higher than that for bare BiFeO<sub>3</sub>, demonstrating that the as-prepared heterostructure can be effectively used as a high-efficiency photocatalyst for antibiotic elimination.

#### Investigation of Photocatalytic Activity Towards Different Pharmaceutical: Isoniazid Degradation

The synergetic adsorption and photocatalytic removal efficiency of the as-prepared composite catalyst was investigated towards another pharmaceutical isoniazid (C<sub>6</sub>H<sub>7</sub>N<sub>3</sub>O) which is often used as a first-line drug in the prevention and treatment of tuberculosis disease [25]. In literature, few studies showed that this persistent drug could be degraded by using TiO<sub>2</sub>, ZnO, Bi<sub>2</sub>O<sub>3</sub> type catalysts under light illumination [26]. Therefore, it is essential to examine the removal of these kinds of pharmaceuticals from aqueous media. In this work, the adsorptive removal of isoniazid by the raw co-polymer seeds was also examined under dark conditions. According to the obtained results shown in Figure 6, the adsorptive removal of isoniazid over the co-STR/DVB polymer was calculated as 80.0% at the of 120 min. The high adsorptive behavior could be related with the interaction of carbonyl groups of isoniazid molecule with the sulfonated aromatic co-polymer structure. It was reported that the hydrogen bonding interactions through the ring nitrogen, the amino nitrogen, and the carbonyl oxygen groups of isoniazid played a dominant role in its adsorption mechanism [27]. Moreover, the isoniazid molecule might be adsorbed on co-STR/DVB through  $\pi$ - $\pi$  stacking effects. On the other hand, raw BFO perovskite showed low degradation efficiency towards isoniazid molecule and only 26% degradation was occurred after 120 min of UV-A light irradiation. Interestingly, the BFO@co-STR/DVB (2:10) catalyst exhibited relatively higher removal rate as 98.2% thanks to the synergetic effect of adsorption and photocatalysis.

#### Cost Estimation of TC Removal in BFO@co-STR/DVB Photocatalytic System

Since cost of the wastewater treatment is a significant factor for photocatalytic and adsorption processes, an economic estimation of applied BFO@co-STR/DVB catalytic system was developed for the tetracycline elimination by considering industrial grade prices of reagents used in the preparation of photocatalyst. The optimum degradation percentage as 98% over BFO@co-STR/DVB was selected with the volume of 50 mL. Table 2 represents the total cost of the reagent consumptions of BFO@co-STR/DVB system which was calculated as \$12.87/m<sup>3</sup>. The cost of the wastewater treatment in this system was calculated much lower than treatment of pharmaceutical wastewater with Fe-TiO<sub>2</sub> system (\$71/m<sup>3</sup>) [28] and caffeine degradation with fenton oxidation process on zeolite supported iron particles (\$23.2m<sup>3</sup>) [29].

**Table 2.** Cost of wastewater treatment per cubic water with BFO@co-STR/DVB system

	Quantity consumed for 1 m <sup>3</sup> (kg/m <sup>3</sup> )	Unit cost (\$/kg)	Total cost (\$/m <sup>3</sup> )
Bi(NO <sub>3</sub> ) <sub>3</sub> ·5H <sub>2</sub> O	0.22	35	7.7
FeCl <sub>3</sub> ·6H <sub>2</sub> O	0.154	20	3.08
NaOH	2.64	0.15	0.39
co-STR/DVB	0.17	10	1.7
Total	12.87		

## CONCLUSION

In this study, perovskite type BiFeO<sub>3</sub> particles were successfully immobilized over copolymer styrene-divinyl benzene surface through simple impregnation method. SEM images with EDX spectrum demonstrated the presence of BiFeO<sub>3</sub> particles on the copolymer surface. FTIR analysis indicated that the deposition did not alter the surface functional groups of co-polymer network. The adsorption abilities of the raw co-polymer were investigated in dark conditions by performing kinetic tests and the results revealed that the robust adsorption occurred between the antibiotic and functional groups of co-STR/DVB structure. The as-prepared composite catalyst showed outstanding removal performance towards tetracycline molecule via synergetic effect of adsorption and photocatalysis. The increasing perovskite ratio on the polymer first increased the removal rate while after certain amount the removal was decreased due to the hindered interaction and adsorption of antibiotic molecules with the co-polymer surface. The composite catalyst was also utilized in another pharmaceutical namely isoniazid and effective adsorptive and photocatalytic behavior was assigned to the mutual effect of carbonyl groups of isoniazid molecule with the sulfonated aromatic co-polymer. This study showed efficient utilization of highly adsorptive co-polymer structure in heterogeneous catalytic processes.

## DATA AVAILABILITY STATEMENT

The authors confirm that the data that supports the findings of this study are available within the article. Raw data that support the finding of this study are available from the corresponding author, upon reasonable request.

## CONFLICT OF INTEREST

The authors declared no potential conflicts of interest with respect to the research, authorship, and/or publication of this article.

## ETHICS

There are no ethical issues with the publication of this manuscript.

## REFERENCES

- [1] V. Dutta, S. Sharma, P. Raizada, A. Hosseini-Bandegharai, J. Kaushal, and P. Singh, "Fabrication of visible light active BiFeO<sub>3</sub>/CuS/SiO<sub>2</sub> Z-scheme photocatalyst for efficient dye degradation," *Materials Letters*, Vol. 270, pp. 2–5, 2020. [\[CrossRef\]](#)
- [2] J. Ćirković, A. Radojković, D. Luković Golić, N. Tasić, M. Čizmić, G. Branković, and Z. Branković, "Visible-light photocatalytic degradation of Mordant Blue 9 by single-phase BiFeO<sub>3</sub> nanoparticles," *Journal of Environmental Chemical Engineering*, Article 104587, 2020. [\[CrossRef\]](#)
- [3] C. Ponraj, G. Vinitha, and J. Daniel, "A review on the visible light active BiFeO<sub>3</sub> nanostructures as suitable photocatalyst in the degradation of different textile dyes," *Environmental Nanotechnology, Monitoring & Management*, Vol. 7, pp. 110–120, 2017. [\[CrossRef\]](#)
- [4] H. Iboukhoulef, R. Douani, A. Amrane, A. Chaouchi, and A. Elias, "Heterogeneous Fenton like degradation of olive Mill wastewater using ozone in the presence of BiFeO<sub>3</sub> photocatalyst," *Journal of Photochemistry and Photobiology A: Chemistry*, Vol. 383, Article 112012, 2019. [\[CrossRef\]](#)
- [5] S. Wu, Y. Lin, C. Yang, C. Du, Q. Teng, Y. Ma, D. Zhang, L. Nie, and Y. Zhong, Enhanced activation of peroxymonosulfate by LaFeO<sub>3</sub> perovskite supported on Al<sub>2</sub>O<sub>3</sub> for degradation of organic pollutants. *Chemosphere* Vol. 237, Article 124478, 2019. [\[CrossRef\]](#)
- [6] H. Li, J. Zhu, P. Xiao, Y. Zhan, K. Lv, L. Wu, and M. Li, "On the mechanism of oxidative degradation of rhodamine B over LaFeO<sub>3</sub> catalysts supported on silica materials: Role of support," *Microporous and Mesoporous Materials*, Vol. 221, pp. 159–166, 2015. [\[CrossRef\]](#)
- [7] A. Alpay, Ö. Tuna, and E.B. Simsek, "Deposition of perovskite-type LaFeO<sub>3</sub> particles on spherical commercial polystyrene resin: A new platform for enhanced photo-Fenton-catalyzed degradation and simultaneous wastewater purification," *Environmental Technology Innovation*, Vol. 20, pp. 101175, 2020. [\[CrossRef\]](#)
- [8] O. Suarez, J.J. Olaya, and S.E. Rodil, "Structural and electrochemical characterization of sulfonated styrene-divinyl benzene/Bismuth-Tin electrodes," *Colloids and Surfaces A: Physicochemical and Engineering Aspects*, Vol. 627, Article 126975. [\[CrossRef\]](#)
- [9] A. Gouthaman, R.S. Azarudeen, A. Gnanaprakasam, V.M. Sivakumar, and M. Thirumarimurugan, "Polymeric nanocomposites for the removal of Acid red 52 dye from aqueous solutions: Synthesis, characterization, kinetic and isotherm studies," *Ecotoxicology and Environmental Safety*, Vol. 160, pp. 42–51, 2018. [\[CrossRef\]](#)

- [10] L. Mohammadi, A. Rahdar, R. Khaksefidi, A. Ghamkhari, G. Fytianos, and G. Z. Kyzas, "Polystyrene magnetic nanocomposites as antibiotic adsorbents," Vol. 12, pp. 1313, 2020. [\[CrossRef\]](#)
- [11] M. Akbulut Söylemez, and B.Ö. Kemaloğulları, "Surface modification of magnetic nanoparticles via admicellar polymerization for selective removal of tetracycline from real water samples, New Journal of Chemistry, Vol. 45, pp. 6415–6423, 2021. [\[CrossRef\]](#)
- [12] M. Qiao, M.M. Wang, M.L. Chen, and J.H. Wang, "A novel porous polymeric microsphere for the selective adsorption and isolation of conalbumin," Analytica Chimica Acta, Vol. 1148, Article 238176, 2021. [\[CrossRef\]](#)
- [13] P. Ergenekon, E. Gürbulak, and B. Keskinler, "Polyol derived sulfonated solvothermal carbon for efficient dye removal from aqueous solutions," Journal of Molecular Liquids, Vol. 50, pp. 16–21, 2011.
- [14] Y. Zhang, K. Chen, B. Gong, Y. Yin, S. Zhou, and K. Xiao, "Scalable synthesis of monodisperse and recyclable sulphonated polystyrene microspheres for sustainable elimination of heavy metals in wastewater," Environmental Technology (United Kingdom), pp. 1–13, 2021. [\[CrossRef\]](#)
- [15] E. Córdova-Mateo, O. Bertran, C.A. Ferreira, and C. Alemán, Transport of hydronium ions inside poly(styrene-co-divinyl benzene) cation exchange membranes, Journal of Membrane Science, Vol. 428, pp. 393–402, 2013.
- [16] T.A. Rauf, and T.S. Anirudhan, "Synthesis and characterization of sulphonic acid ligand immobilized Aminopropyl silanetriol copolymer and evaluation of its Bovine serum albumin adsorption efficiency," Materials Today: Proceedings, Vol. 41, pp. 728–735, 2020. [\[CrossRef\]](#)
- [17] L. Wang, J.B. Xu, B. Gao, A.M. Chang, J. Chen, L. Bian, and C.Y. Song, "Synthesis of BiFeO<sub>3</sub> nanoparticles by a low-heating temperature solid-state precursor method," Materials Research Bulletin, Vol. 48, pp. 383–388, 2013. [\[CrossRef\]](#)
- [18] N.S. Abdul Satar, R. Adnan, H.L. Lee, S.R. Hall, T. Kobayashi, M.H. Mohamad Kassim, and N.H. Mohd Kaus, "Facile green synthesis of yttrium-doped BiFeO<sub>3</sub> with highly efficient photocatalytic degradation towards methylene blue," Ceramics International, Vol. 45, pp. 15964–15973, 2019. [\[CrossRef\]](#)
- [19] M. Mahmoud Nasef, H. Saidi, and K.Z. Mohd Dahlan, "Kinetic investigations of graft copolymerization of sodium styrene sulfonate onto electron beam irradiated poly(vinylidene fluoride) films," Radiation Physics and Chemistry, Vol. 80, pp. 66–75, 2011. [\[CrossRef\]](#)
- [20] L. Melo, R. Benavides, G. Martínez, L. Da Silva, and M.M.S. Paula, "Degradation reactions during sulphonation of poly(styrene-co-acrylic acid) used as membranes," Polymer Degradation Stability, Vol. 109, pp. 343–352, 2014. [\[CrossRef\]](#)
- [21] Z. Balta, E.B. and Simsek, "Uncovering the systematical charge separation effect of boron nitride quantum dots on photocatalytic performance of BiFeO<sub>3</sub> perovskite towards degradation of tetracycline antibiotic," Journal of Environmental Chemical Engineering, Vol. 9, Article 106567, 2021. [\[CrossRef\]](#)
- [22] J. Yang, L. Han, W. Yang, Q. Liu, Z. Fei, X. Chen, Z. Zhang, J. Tang, M. Cui, X. Qiao, "In situ synthetic hierarchical porous MIL-53(Cr) as an efficient adsorbent for mesopores-controlled adsorption of tetracycline," Microporous and Mesoporous Materials, Vol. 332, Article 111667, 2022. [\[CrossRef\]](#)
- [23] M. Sharma, J. Singh, S. Hazra, and S. Basu, Adsorption of heavy metal ions by mesoporous ZnO and TiO<sub>2</sub>@ZnO monoliths: Adsorption and kinetic studies, Microchemical Journal, Vol. 145, pp. 105–112, 2019. [\[CrossRef\]](#)
- [24] T.T.N. Phan, A.N. Nikoloski, P.A. Bahri, and D. Li, "Enhanced removal of organic using LaFeO<sub>3</sub>-integrated modified natural zeolites via heterogeneous visible light photo-Fenton degradation," Journal of Environmental Management, Vol. 233, pp. 471–480, 2019. [\[CrossRef\]](#)
- [25] E. Carazo, A. Borrego-Sánchez, F. García-Villén, R. Sánchez-Espejo, C. Viseras, P. Cerezo, and C. Aguzzi, "Adsorption and characterization of palygorskite-isoniazid nanohybrids," Applied Clay Science, Vol. 160, pp. 180–185, 2018. [\[CrossRef\]](#)
- [26] R.R.S. Coronado-Castañeda, M.L. Maya-Treviño, E. Garza-González, J. Peral, M. Villanueva-Rodríguez, and A. Hernández-Ramírez, "Photocatalytic degradation and toxicity reduction of isoniazid using β-Bi<sub>2</sub>O<sub>3</sub> in real wastewater," Catal Today, vol. 341, pp. 82–89, 2020. [\[CrossRef\]](#)
- [27] S. Akyuz, T. Akyuz, and E. Akalin, "Adsorption of isoniazid onto sepiolite-palygorskite group of clays: An IR study," Spectrochimica Acta Part A-molecular and Biomolecular Spectroscopy, Vol. 75, pp. 1304–1307, 2010. [\[CrossRef\]](#)
- [28] P. Bansal, A. Verma, and S. Talwar, "Detoxification of real pharmaceutical wastewater by integrating photocatalysis and photo-Fenton in fixed-mode," Chemical Engineering Journal, Vol. 349, pp. 838–848, 2018. [\[CrossRef\]](#)
- [29] M. Anis, and S. Haydar, "Heterogeneous fenton oxidation of caffeine using zeolite-supported iron nanoparticles," Arabian Journal for Science and Engineering, Vol. 44, pp. 315–328, 2019. [\[CrossRef\]](#)